

Semi-parametric Benchmark Dose Analysis with Monotone Additive Models

Alex Stringer¹, Tugba Akkaya-Hocagil¹, Richard Cook¹, Louise Ryan²,
Sandra W. Jacobson³, and Joseph L. Jacobson³

¹Department of Statistics and Actuarial Science, University of Waterloo,
Waterloo, Canada

²School of Mathematics and Statistics, University of Technology Sydney

³Department of Psychiatry and Behavioural Neurosciences, Wayne State
University School of Medicine

Abstract

Benchmark dose analysis aims to estimate the level of exposure to a toxin that results in a clinically-significant adverse outcome and quantifies uncertainty using the lower limit of a confidence interval for this level. We develop a novel framework for benchmark dose analysis based on monotone additive dose-response models. We first introduce a flexible approach for fitting monotone additive models via penalized B-splines and Laplace-approximate marginal likelihood. A reflective Newton method

is then developed that employs de Boor’s algorithm for computing splines and their derivatives for efficient estimation of the benchmark dose. Finally, we develop and assess three approaches for calculating benchmark dose lower limits: a naive one based on asymptotic normality of the estimator, one based on an approximate pivot, and one using a Bayesian parametric bootstrap. The latter approaches improve upon the naive method in terms of accuracy and are guaranteed to return a positive lower limit; the approach based on an approximate pivot is typically an order of magnitude faster than the bootstrap, although they are both practically feasible to compute. We apply the new methods to make inferences about the level of prenatal alcohol exposure associated with clinically significant cognitive defects in children using data from an NIH-funded longitudinal study. Software to reproduce the results in this paper is available at <https://github.com/awstringer1/bmd-paper-code>.

1 Introduction

1.1 Benchmark dose analysis

Methodology for benchmark dose analysis is used by environmental toxicologists to quantify the level of exposure to a harmful substance associated with an adverse response. The US Environmental Protection Agency (EPA, 2012) and the European Food Safety Authority (EFSA et al., 2022) use the lower limit of a 95% confidence interval of the *benchmark dose*—called the benchmark dose, lower (BMDL)—to set limits on acceptable levels of exposure to a wide variety of toxic substances. In this paper we present a flexible and general computational and inferential framework for benchmark dose analysis and inference based on monotone

additive models. We apply the new methodology to the problem of estimating levels of prenatal alcohol exposure that are associated with clinically significant cognitive defects in children.

Crump (1984, 1995) introduced the concept of a benchmark dose (BMD) and recommended using the lower limit of a confidence interval for it (BMDL) to define the acceptable exposure to a toxic substance. Methods were developed first for parametric dose-response modeling of data obtained from designed experiments. Budtz-Jorgensen et al. (2001) proposed a dose-response model based on a continuous exposure obtained from epidemiological (observational) studies that incorporates a propensity score-based adjustment for confounders. They derive an exact confidence interval for the BMD estimator based on a linear dose-response model with Gaussian errors. In recent work on parametric dose-response models, Aerts et al. (2020) defined a family of parametric dose-response functions and recommended model-averaged point estimates based on a computationally intensive bootstrap procedure.

It has been argued that parametric dose-response modeling is not sufficiently flexible for the task of setting benchmark doses leading to the development of various semi- and non-parametric approaches. Wheeler and Bailer (2012) use Gibbs sampling to fit models based on monotone P-splines in a Bayesian framework that requires model-specific calculations, intensive computations, and manual convergence tuning and assessment. For binary outcomes, non-parametric methods were developed by Piegorsch et al. (2012, 2014) using isotonic regression for dose-response modelling, again relying on intensive bootstrap calculations for BMDL estimation; methods to deal with continuous responses were developed by Lin et al. (2015). Wheeler et al. (2015) present a non-parametric quantile regression-

based method. These procedures are all characterized by their completely non-parametric dose-response models, and associated computationally-intensive inference procedures.

1.2 Contributions

We take a semi-parametric approach to benchmark dose analysis, combining the efficiency of the parameteric approaches with the flexibility of the non-parameteric methods. Our approach uses monotone generalized additive models to estimate the benchmark dose and calculate the BMDL; the restriction to estimation of monotone dose-response curves reflects the assumption that an increased exposure cannot yield a less adverse average response (Wheeler and Bailer, 2012). We introduce a novel procedure for fitting monotone generalized additive models based on B-splines with coefficients parameterized to yield estimates of a monotone curve. Laplace-approximate marginal likelihood (Wood, 2011) is applied for smoothing parameter selection and uncertainty quantification (Wood et al., 2016). We then develop a fast and stable method for solving the (random) non-linear equation defining the BMD estimate based on de Boor’s algorithm for B-splines and their derivatives (de Boor, 2001), made feasible by deriving bounds on the estimated BMD and then applying a reflective Newton line search. Finally, we introduce three methods for BMDL calculation: a) a “Delta method” lower limit based on asymptotic normality of the estimated BMD, b) inversion of a hypothesis test based on an approximate pivot obtained from the estimating equation defining the BMD using another reflective Newton procedure, and c) a Bayesian parametric bootstrap based on asymptotic normality of the maximum likelihood estimator. The Delta method is fast but typically too conservative (coverage higher than nominal; see Table 1

in Section 4) and may give BMDLs that lie below zero exposure, providing no information about the BMD. The approximate pivot-based BMDL solves this problem, and is nearly as fast due to the development of a second de Boor/Newton algorithm. Further, the speed of the novel BMD estimation algorithm make the parametric bootstrap approach computationally feasible in typical applications.

1.3 Motivating application

Prenatal alcohol exposure (PAE) has been linked to a broad range of long-term cognitive and behavioral deficits (Jacobson et al., 2023). However, there is relatively little information about the *level* of PAE that is associated with clinically significant cognitive deficits. Attempts to define what constitutes excessive drinking have been both qualitative (Stratton et al., 1996; Hoyme, 2005; Chudley et al., 2005; Cook et al., 2016) and quantitative (Astley and Clarren, 2000; Hoyme et al., 2016), although Astley and Clarren (2000) emphasize that there is no “clear consensus on the amount of alcohol that can actually be toxic to the fetus”. Addressing this question has important clinical implications in terms of diagnosing children who have been adversely affected by pre-natal alcohol exposure. We apply our method for semi-parametric benchmark dose analysis to this problem using data from six United States National Institutes of Health-funded longitudinal studies in which expectant women were interviewed regarding their drinking behaviour during pregnancy and their children followed through young adulthood and assessed using a variety of cognitive tests.

2 Benchmark Dose Analysis and Monotone Splines

2.1 Benchmark dose analysis

Consider a response $Y_i \in \mathbb{R}$, let $x_i \in \mathbb{R}$ represent the exposure for individual $i = 1, \dots, n$ in a sample of size n . We consider the following dose-response model:

$$Y_i = \alpha + f(x_i) + \sum_{j=1}^m g_j(z_{ij}) + \sigma \epsilon_i, \quad \epsilon_i \stackrel{\text{iid}}{\sim} \text{N}(0, 1), \quad i = 1, \dots, n, \quad (1)$$

where α is an intercept, $f(x)$ is a strictly monotone decreasing function of the exposure, and $g_j(z_j)$ are m functions of further covariates, z_j , for $j = 1, \dots, m$. This specification assumes that an increase in x reduces the mean response, appropriate for settings where smaller values of the response are considered more adverse, as is the case with cognition scores.

We let $x_{\mathbf{b}}$ represent the exposure level that yields a specified increase—called the benchmark response (BMR, denoted as p_+)—in the probability of a response falling below a specified threshold; see Crump (1995) and Akkaya Hocagil et al. (2023) for detailed discussion of what follows. If $p_0 \in (0, 1)$, let $p_+ \in (0, 1 - p_0)$, and $\tau_0(x_0, z)$ satisfy $\mathbb{P}(Y < \tau_0(x_0, z); x_0, z) = p_0$ where $\mathbb{P}(\cdot; x, z)$ is the probability distribution for Y following the model (1) with covariates (x, z) . Here $x_0 \in \mathbb{R}$ is a baseline exposure and is almost always set at $x_0 = 0$ in practice, representing an unexposed subject. The benchmark dose (BMD, denoted as $x_{\mathbf{b}}$) is defined as the value of x satisfying

$$\mathbb{P}(Y < \tau_0(x_0, z); x_{\mathbf{b}}, z) = p_0 + p_+. \quad (2)$$

Under the additive model (1), $x_{\mathbf{b}}$ is defined by the nonlinear equation $U(x_{\mathbf{b}}) = 0$, where

$$U(x) = (f(x_0) - f(x)) / \sigma - c(p_0, p_+), \quad (3)$$

and $c(p_0, p_+) = \Phi^{-1}(p_0 + p_+) - \Phi^{-1}(p_0)$ where $\Phi(\cdot)$ is the standard normal cumulative distribution function. It is clear from (3) that defined this way, x_b does not depend on $\tau_0(x_0, z)$ or z . An estimate, \hat{x}_b , of x_b solves the nonlinear equation $U_n(\hat{x}_b) = 0$, where

$$U_n(x) = \left(\hat{f}(x_0) - \hat{f}(x) \right) / \hat{\sigma} - c(p_0, p_+), \quad (4)$$

and $\hat{f}(x), \hat{\sigma}$ are estimates of $f(x)$ and σ .

2.2 Quantifying uncertainty in the benchmark dose

To address the uncertainty in estimation of the benchmark dose it is common to base guidelines on a lower limit of the benchmark dose (or benchmark dose-lower; BMDL), defined as the lower endpoint of an approximate 95% confidence interval for x_b . Budtz-Jorgensen et al. (2001) derive the exact sampling distribution of \hat{x}_b in linear dose-response models and use it to give a formula for a BMDL. The explicit sampling distribution of \hat{x}_b is not available in more flexible dose-response models, and a common approach is to make inferences based on the Delta method, relying on asymptotic normality of \hat{x}_b . Computationally-intensive bootstrap-based BMDL estimation is also possible; see Moerbeek et al. (2004) for a review of existing methods. We derive these methods, as well as one additional method for uncertainty quantification of the BMD based on semi-parametric dose-response models in Section 3.4.

2.3 Monotone B-splines

The dose-response function is represented as a monotone spline function, which proves useful for both fitting the dose-response model and rapid computation of the BMD and BMDL,

and also ensures that a BMD exists for some choice of the BMR; see Section 3. The function $f(x)$ can be written as

$$f(x) = \sum_{l=1}^L b_{l,p}(x)\beta_l, \quad (5)$$

where $b_{l,p}(x)$ is the l^{th} B-spline function of order p on the interval $[a, b] \subset \mathbb{R}$ with knots $\mathbf{t} = (t_1, \dots, t_{L+p})$ such that $a \leq t_1 \leq \dots \leq t_{L+p} \leq b$. Using cubic B-splines having $p = 4$, we follow the standard practice of choosing a large value of L and controlling over-fitting through penalized estimation; see Wood et al. (2016); Wood (2017) for details.

Note that B-splines are defined recursively with $b_{l,1}(x) = I([t_l, t_{l+1}))$ and $b_{l,p}(x) = \omega_{l,p-1}b_{l,p-1}(x) + (1 - \omega_{l+1,p-1})b_{l+1,p-1}(x)$ where $\omega_{l,p}(x) = (x - t_l)/(t_{l+p} - t_l)I(t_{l+p} \neq t_l)$. These definitions are used during model fitting (Section 3.2) to compute the design matrix where the x at which the splines are to be evaluated are specified in advance.

The numerical methods of Section 3 (see also Algorithms 2 and 3 in Appendix A) require computation of the entire spline function (5) within an iterative root-finding procedure at many values of x that cannot be known in advance. In this setting, computing $b_{1,p}(x), \dots, b_{L,p}(x)$ naively and computing $f(x)$ using (5) is too computationally intensive, since this wastefully ignores the fact that only $p + 1 \ll L$ of the basis functions are non-zero for each x . de Boor's algorithm (de Boor, 2001) computes the entire spline function $f(x)$ efficiently by avoiding computation of the individual basis functions $b_{l,p}(x)$, and ignoring computations known to add zero to the overall sum; see Algorithm 1 in Appendix A. This greatly increases the speed of the computations involved in estimating the BMD and hence makes the parametric bootstrap of Section 3.4 practically feasible.

The derivative of a B-spline basis function is given by $b'_{l,p}(x) = (p - 1)(b'_{l,p-1}(x)/(t_{l+p-1} -$

$t_l) - b'_{l+1,p-1}(x)/(t_{l+p} - t_{l+1}))$, and the derivative of the entire spline function (5) is:

$$f'(x) = (p - 1) \sum_{l=2}^L b_{l,p-1}(x) \frac{\beta_l - \beta_{l-1}}{t_{l+p-1} - t_l}. \quad (6)$$

From this it can be seen that $\beta_1 < \dots < \beta_L$ is a sufficient condition for $f(x)$ to be strictly monotone decreasing, and this is straightforward to ensure during model fitting via re-parameterization as introduced by Pya and Wood (2015); see Section 3.2. Further, because the derivatives of a spline function are also spline functions (linear combinations of spline basis functions), de Boor’s algorithm is also applied to obtain the derivatives required to implement Newton’s method, leading to further computational benefits.

3 Inferences about the Benchmark Dose

3.1 Existence of the benchmark dose

The benchmark dose x_b , defined as the solution to $U(x) = 0$ where $U(x)$ is given by (2), is not guaranteed to exist for every choice of x_0, p_0, p_+ . The specification of x_0, p_0, p_+ should be context-dependent; see Haber et al. (2018). We repeat that $x_0 = 0$ is almost always specified, representing an unexposed subject.

Assumption 1 is sufficient to ensure that for some p_0, p_+ , there exists a value of x_b satisfying $U(x_b) = 0$:

Assumption 1 (a) *The unknown function $f(x)$ is continuously differentiable with $\sup_{x \in \mathbb{R}} |f'(x)| < \infty$ and $f'(x) < 0$ for every $x \in \mathbb{R}$; and (b) with probability 1 the estimated function $\hat{f}(x)$ is continuously differentiable with $\sup_{x \in \mathbb{R}} |\hat{f}'(x)| < \infty$ and $\hat{f}'(x) < 0$ for every $x \in \mathbb{R}$.*

Assumption 1 (a) states that higher exposure cannot be associated with an equal or better expected response. Assumption 1 (b) can be satisfied by applying a monotonic smoother, as we do in Sections 2.3 and 3.2. Since $U(x_0) < 0$ from Assumption 1, by the intermediate value theorem $U(x_{\max}) > 0$ is a sufficient condition for the existence of $x_{\mathbf{b}} \in (x_0, x_{\max})$ satisfying $U(x_{\mathbf{b}}) = 0$. Further, a sufficient condition for the estimate $\widehat{x}_{\mathbf{b}}$ to exist is $U_n(x_{\max}) > 0$. In practice, we recommend to check $U_n(x_{\max}) > 0$, and decrease p_+ if this condition is not satisfied. In cases where the underlying dose-response curve is not monotonic, a benchmark dose may not exist, and this is important to consider in applications.

3.2 Fitting the dose-response model

Under the B-spline representation (5), the dose-response model (1) is:

$$Y_i = \alpha + \sum_{l=1}^L b_{l,4}(x_i)\beta_l^c + \sum_{j=1}^m \sum_{l=1}^L b_{l,4}(z_{ij})\gamma_{jl} + \sigma\epsilon_i, \quad \epsilon_i \stackrel{\text{iid}}{\sim} \text{N}(0, 1), \quad i = 1, \dots, n. \quad (7)$$

Monotonicity can be enforced by reparameterization Pya and Wood (2015). We set $\beta_1^c = \beta_1$ and $\beta_l^c = \beta_{l-1}^c - \exp(\beta_l)$, $l = 2, \dots, L$, which guarantees that $\beta_1^c < \dots < \beta_L^c$ and hence that $f(x)$ and its estimate, $\widehat{f}(x) = b_{1,4}(x)\widehat{\beta}_1^c + \dots + b_{L,4}(x)\widehat{\beta}_L^c$, are monotone decreasing. The unknown parameters to be estimated are $\boldsymbol{\Psi} = (\alpha, \boldsymbol{\beta}, \boldsymbol{\gamma}) \in \mathbb{R}^D$ where $\alpha \in \mathbb{R}$, $\boldsymbol{\beta} = (\beta_1, \dots, \beta_L) \in \mathbb{R}^L$, and $\boldsymbol{\gamma} = (\gamma_{11}, \dots, \gamma_{mL}) \in \mathbb{R}^{mL}$, so that $D = 1 + L(1 + m)$.

We define the design matrices $\mathbf{B} = (B_{il})$ with $B_{il} = b_{l,4}(x_i)$ and $\mathbf{Z} = [\mathbf{Z}_1 : \dots : \mathbf{Z}_m]$ with $\mathbf{Z}_j = (Z_{jil})$ and $Z_{jil} = b_{l,4}(z_{ij})$, and define $\boldsymbol{\phi} = (\tau, \boldsymbol{\lambda}) \in \mathbb{R}^s$ where $s = m + 2$, $\tau = -2 \log \sigma$, and $\boldsymbol{\lambda} = (\lambda_1, \dots, \lambda_{m+1})$ where $\lambda_j \in \mathbb{R}$ are (log) smoothing penalty parameters to be estimated. Finally, let $\mathbf{S}_1, \mathbf{S}_2, \dots, \mathbf{S}_{m+1}$ be matrices of integrated squared second B-spline derivatives, computed according to the algorithm of Wood (2017), and let $\mathbf{S}_{\boldsymbol{\lambda}} =$

$\text{diag}(e^{\lambda_2} \mathbf{S}_2, \dots, e^{\lambda_{m+1}} \mathbf{S}_{m+1})$. A penalized joint (negative) log-likelihood for the unknown parameters, (Ψ, ϕ) , is

$$\ell(\Psi, \phi) = \frac{1}{2} e^\tau \|\mathbf{y} - \alpha \mathbf{1}_n - \mathbf{B}\beta_c - \mathbf{Z}\gamma\|_2^2 + e^{\lambda_1} \beta^\top \mathbf{S}_1 \beta + \gamma^\top \mathbf{S}_\lambda \gamma, \quad (8)$$

and a marginal likelihood for ϕ is

$$\mathcal{L}(\phi) = \int \exp\{-\ell(\Psi, \phi)\} d\Psi. \quad (9)$$

We define the profile maximum likelihood estimator as $\widehat{\Psi}(\phi) = \text{argmin}_{\Psi} \ell(\Psi, \phi)$, and the Hessian matrix $\mathbf{H}(\phi) = -\partial_{\Psi}^2 \ell(\widehat{\Psi}(\phi), \phi)$. Inferences about ϕ are to be based on the Laplace-approximate maximum marginal likelihood estimator, $\widehat{\phi} = \text{argmax}_{\phi} \mathcal{L}_{\text{LA}}(\phi)$, where

$$\mathcal{L}_{\text{LA}}(\phi) = (2\pi)^{D/2} |\mathbf{H}(\phi)|^{-1/2} \exp\{-\ell(\widehat{\Psi}(\phi), \phi)\} \quad (10)$$

is a Laplace approximation to $\mathcal{L}(\phi)$. Point estimates of Ψ are then given as $\widehat{\Psi}(\widehat{\phi})$, and a point estimate of the unknown dose-response function at any $x \in \mathbb{R}$ is $\widehat{f}(x) = b(x)^\top \widehat{\beta}_c$ with $b(x) = (b_{1,A}(x), \dots, b_{L,A}(x))^\top$. Estimates \widehat{g}_j for each $g_j, j = 1, \dots, m$ are analogously obtained. Uncertainty quantification is discussed in Section 3.4.

Spline calculations are carried out using the Rcpp framework (Eddelbuettel and Francois, 2011). The Template Model Builder (TMB) framework (Kristensen et al., 2016) is used for automatic differentiation and Laplace approximation, yielding efficient computation of $\log \mathcal{L}_{\text{LA}}(\phi)$ and $\partial_{\phi} \log \mathcal{L}_{\text{LA}}(\phi)$. We compute $\widehat{\phi}$ via quasi-Newton optimization based on these quantities. The linear constraints $\sum_{i=1}^n \widehat{f}(x_i) = 0$ and $\sum_{i=1}^n \widehat{g}(z_{ij}) = 0, j = 1, \dots, m$ are imposed directly, to avoid ‘‘constraint-absorbing’’ reparameterizations (Stringer, 2023). Note that because $U_n(\cdot)$ is invariant to the addition of constant terms to \widehat{f} , estimation of x_b is

invariant to the choice of linear constraints. However, such constraints are required to ensure the identifiability of α as well as more than one f and g together, so they still must be used.

3.3 Computational method for benchmark dose estimation

Given a fitted dose-response model, we obtain the estimate, \hat{x}_b , defined as the solution to a non-linear equation, $U_n(\hat{x}_b) = 0$, via a reflective Newton line search. The efficiency and stability of the method is critically important in the parametric bootstrap of Section 3.4 where we repeat the procedure thousands of times to calculate a benchmark dose lower limit. Efficient computation of the required B-spline functions and derivatives to implement the Newton iteration is facilitated by de Boor's algorithm, and a stable iteration is achieved by bounding the solution to a known interval.

Bounds on \hat{x}_b are obtained by noting that Assumption 1 (b) guarantees that $U_n(\cdot)$ is continuous and strictly monotonic, and further that $U_n(x_0) = -c(p_0, p_+) < 0$. We therefore check the condition that $U_n(x_{\max}) > 0$ in applications. If this constraint is satisfied, then by definition of \hat{x}_b and the intermediate value theorem, $x_0 < \hat{x}_b < x_{\max}$. We then augment the typical Newton iteration with the reflective transformation given by Coleman and Li (1994), using (x_0, x_{\max}) as the required interval within which the solution is known to lie. The full algorithm is given in Algorithm 2 in the Appendix, which depends further on de Boor's algorithm (Algorithm 1).

3.4 Computation of benchmark dose lower limits

Inferences about x_b are based on a benchmark dose lower limit, \hat{x}_1 , defined as the lower endpoint of a 95% confidence interval for x_b ; see Section 2.2. Here we introduce three candidate lower limits: one based on a Bayesian parametric bootstrap, one based on the Delta method for \hat{x}_b , and one based on an approximate pivot obtained from U_n .

3.4.1 Bayesian parametric bootstrap

To quantify uncertainty in the estimated regression coefficients from the dose-response model, $\hat{\Psi}$, and functions of them including the estimated BMD, \hat{x}_b , we consider inference based on (approximate) posterior samples in a Bayesian framework; see Wood et al. (2016) for a detailed exposition. For notational clarity, denote the entire vector of spline weights and variance/smoothing parameters by $\boldsymbol{\theta} = (\boldsymbol{\Psi}, \boldsymbol{\phi})$, with estimate $\hat{\boldsymbol{\theta}} = (\hat{\boldsymbol{\Psi}}, \hat{\boldsymbol{\phi}})$. Given $\hat{\boldsymbol{\theta}}$, we employ the approximation $\boldsymbol{\theta}|\mathbf{Y} \sim \mathbf{N}(\hat{\boldsymbol{\theta}}, \mathbf{H}^{-1}(\hat{\boldsymbol{\phi}}))$. We draw samples, $\{\boldsymbol{\theta}_j\}_{j=1}^M$ where $M \in \mathbb{N}$, from $\boldsymbol{\theta}|\mathbf{Y}$ using the method of Rue (2001), based on the Cholesky decomposition of $\mathbf{H}(\hat{\boldsymbol{\phi}})$.

Given $\boldsymbol{\theta}_j$, a sample, $\boldsymbol{\Psi}_j$, from $\boldsymbol{\Psi}|\mathbf{Y}$ is obtained by indexing the first $\dim(\boldsymbol{\Psi})$ components of $\boldsymbol{\theta}_j$; a sample, $\boldsymbol{\phi}_j$, from $\boldsymbol{\phi}|\mathbf{Y}$ is obtained as the remaining $\dim(\boldsymbol{\phi})$ components. Further, a sample, x_b^j , from $x_b|\mathbf{Y}$ is obtained by running Algorithm 2 with $\boldsymbol{\theta}_j$ as the input. The bootstrap BMDL, \hat{x}_1^{boot} , is the 2.5th percentile of the M BMD samples obtained in this manner. This procedure involves running Algorithm 2 M times, and is made computationally feasible by the use of de Boor's algorithm for both \hat{f} and \hat{f}' ; see Algorithm 2. A more naive parametric bootstrap would fit the entire dose-response model (14) M times, but the use of (approximate) posterior samples requires only a single model fit, and hence is

computationally efficient.

3.4.2 Delta method

Although the bootstrap procedure of Section 3.4.1 is fast, a faster Delta-method lower bound is obtained from the frequentist asymptotic approximation:

$$\widehat{\Psi} \sim N\left(\Psi, \mathbf{H}^{-1}(\widehat{\phi})\right). \quad (11)$$

From this, we obtain $U_n(x_{\mathbf{b}})/V_n(x_{\mathbf{b}})^{1/2} \sim N(0, 1)$, where

$$V_n(x_{\mathbf{b}}) = \text{Var}\{U_n(x_{\mathbf{b}})\} = \frac{1}{\widehat{\sigma}^2} (b(x_0) - b(x_{\mathbf{b}}))^{\top} \Sigma(\widehat{\beta}) (b(x_0) - b(x_{\mathbf{b}})),$$

and $\Sigma(\widehat{\beta}) = \text{Cov}(\widehat{\beta})$. A linear Taylor series approximation, $U_n(x_{\mathbf{b}}) \approx U'_n(\widehat{x}_{\mathbf{b}})(x_{\mathbf{b}} - \widehat{x}_{\mathbf{b}})$, gives:

$$\frac{U'_n(\widehat{x}_{\mathbf{b}})}{V_n(\widehat{x}_{\mathbf{b}})^{1/2}} (\widehat{x}_{\mathbf{b}} - x_{\mathbf{b}}) \sim N(0, 1). \quad (12)$$

We obtain samples, β_c^j , from θ_j by indexing out β^j from each and then applying the transformation given in Section 3.2. We use the sample covariance matrix of $\beta_c^1, \dots, \beta_c^M$, $\widehat{\Sigma}(\widehat{\beta}) = \text{Cov}(\beta_c^1, \dots, \beta_c^M)$, to estimate $\Sigma(\widehat{\beta})$. We then compute $V_n(\widehat{x}_{\mathbf{b}})$ directly, using the recursions for B-splines. A Delta method-based BMDL is then:

$$\widehat{x}_1^{\Delta} = \widehat{x}_{\mathbf{b}} - 2 \frac{V_n(\widehat{x}_{\mathbf{b}})^{1/2}}{|U'_n(\widehat{x}_{\mathbf{b}})|}. \quad (13)$$

Computation of $U'_n(\widehat{x}_{\mathbf{b}})$ via de Boor's algorithm is described within Algorithm 2.

3.4.3 Approximate pivot

The Delta method lower bound of Section 3.4.2 is fast to compute, but may be inaccurate and return a lower bound, $\widehat{x}_1^{\Delta} < x_0$, in practice. Such a lower bound provides no information

about $x_{\mathbf{b}}$. We observe such an unusable estimate in a significant proportion of simulations (Table 2 in Section 4); in the application to the PAE study data in Section 5, we find that \widehat{x}_1^Δ is very close to zero and substantially smaller than the other two BMDLs. We address this problem by introducing the approximate pivot-based BMDL, $\widehat{x}_1^{\text{piv}} \in \inf \widehat{\mathcal{C}}_n(\alpha)$, where

$$\widehat{\mathcal{C}}_n(\alpha) = \{x \in \mathbb{R} : U_n(x)^2 < V_n(x)\chi_{1,\alpha}^2\}.$$

This is motivated by the approximate pivot $U_n(x_{\mathbf{b}})^2/V_n(\widehat{x}_{\mathbf{b}}) \sim \chi_1^2$ which follows immediately from $U_n(x_{\mathbf{b}})/V_n(x_{\mathbf{b}})^{1/2} \sim N(0,1)$. However, we do not employ a Delta method, instead relying directly on the approximate distribution of the pivot. This yields accurate intervals that cannot cross zero; see the simulations in Section 4.

Computation of $\widehat{x}_1^{\text{piv}}$ is more involved than that of \widehat{x}_1^Δ . We utilize another application of the reflective Newton line search coupled with de Boor’s algorithm, yielding a procedure nearly as fast as the Delta method and much faster than the bootstrap, as follows. Define the function $\kappa_n(x) = U_n(x)^2 - V_n(x)\chi_{1,\alpha}^2$ and note that $\widehat{x}_1^{\text{piv}} \in \inf \{x : \kappa_n(x) = 0\}$. Accordingly, we use an appropriate modification of Algorithm 2 to find an appropriate zero of κ_n . The required derivative is $\kappa'_n(x) = 2U_n(x)U'_n(x) - V'_n(x)\chi_{1,\alpha}^2$ where $V'_n(x) = -2b'(x)^\top \Sigma(\widehat{\boldsymbol{\beta}}) (b(x_0) - b(x))$. Both the B-spline basis function vectors, $b(x)$, and their vectors of derivatives, $b'(x)$, are computed directly using the recursions described in Section 2.3. Bounds are obtained by observing that $\kappa_n(x_0) = c(p_0, p_+)^2 > 0$ and $\kappa_n(\widehat{x}_{\mathbf{b}}) = -V_n(\widehat{x}_{\mathbf{b}})\chi_{1,\alpha}^2 < 0$, and applying the intermediate value theorem to conclude that there exists $\widehat{x}_1^{\text{piv}} \in (x_0, \widehat{x}_{\mathbf{b}})$. Although such a root may or may not be unique, we have not observed problems with convergence or stability in our experiments (Section 4) or data analysis (Section 5). The full algorithm is given in Algorithm 3 in Appendix A.

4 Empirical Performance and Computational Considerations

We compare via simulations the empirical performance of the three candidate BMDL's: \hat{x}_1^{boot} (Section 3.4.1), \hat{x}_1^Δ (Section 3.4.2), and \hat{x}_1^{piv} (Section 3.4.3). All computations are performed using the `semibmd` R package which implements the methods described in Section 3. We report empirical coverage probabilities and relative computation times for 100,000 replicates simulated under the true dose-response function $f(x) = \exp(-sx)$ for varying $s > 0$. This gives a monotone curve of varying steepness, where smaller s yields a flatter curve and hence a more difficult estimation problem. Table 1 shows the bias and empirical coverage rates of \hat{x}_1^Δ , \hat{x}_1^{piv} , and \hat{x}_1^{boot} , the latter based on 1000 parametric bootstrap replications for each of the 100,000 simulated replicates; since these are lower limits of two-sided 95% confidence intervals, they are expected to yield coverage of approximately 97.5%. The performance of \hat{x}_1^Δ is broadly unsatisfactory: the average coverage is too high in all cases, which includes a substantial proportion of computed lower limits having $\hat{x}_1^\Delta < x_0$; see Table 2. Note that \hat{x}_1^{piv} and \hat{x}_1^{boot} are within 2 standard errors of the nominal coverage in all cases, with the former occasionally slightly lower and the latter occasionally slightly higher.

Table 2 summarizes computational aspects of the procedure. The score method is essentially just as fast as the Delta method, but with the advantage of not being able to return a computed lower bound that is less than x_0 . In contrast, Table 2 shows the percentage of simulations in each configuration that yielded an estimated $\hat{x}_1^\Delta < x_0$, and would therefore be unhelpful in practice. This happens in a substantial proportion of cases, especially at lower sample sizes and for flatter dose-response curves. This can be regarded as a disadvantage of

n	s	σ	EBias	%ECP(\hat{x}_1^Δ)	%ECP(\hat{x}_1^{piv})	%ECP(\hat{x}_1^{boot})
200	.1	.1	5.7(0.06)	100.0(0.00)	94.6(0.07)	100.0(0.00)
		.2	-7.9(0.11)	100.0(0.00)	94.7(0.08)	100.0(0.00)
		.5	-91.8(0.14)	100.0(0.00)	100.0(0.00)	100.0(0.00)
	.5	.1	0.7(0.01)	99.8(0.01)	97.3(0.05)	99.1(0.03)
		.2	3.0(0.03)	99.9(0.01)	97.0(0.05)	99.6(0.02)
		.5	5.7(0.07)	100.0(0.00)	93.4(0.08)	100.0(0.00)
	1	.1	0.2(0.00)	99.5(0.02)	97.0(0.05)	98.5(0.04)
		.2	1.2(0.02)	99.5(0.02)	96.6(0.06)	99.1(0.03)
		.5	5.4(0.04)	100.0(0.01)	96.1(0.06)	99.9(0.01)
	2	.1	0.7(0.02)	98.0(0.04)	95.6(0.06)	97.9(0.05)
		.2	1.5(0.03)	98.1(0.04)	95.8(0.06)	98.8(0.03)
		.5	2.8(0.02)	100.0(0.01)	96.5(0.06)	99.6(0.02)
	5	.1	0.1(0.01)	98.3(0.04)	95.9(0.06)	97.4(0.05)
		.2	0.2(0.01)	99.5(0.02)	96.7(0.06)	98.5(0.04)
		.5	1.2(0.01)	100.0(0.01)	95.9(0.06)	99.1(0.03)
500	.1	.1	3.8(0.04)	99.8(0.02)	97.4(0.05)	100.0(0.01)
		.2	-4.1(0.08)	100.0(0.00)	96.0(0.07)	100.0(0.00)
		.5	-87.5(0.12)	100.0(0.00)	100.0(0.00)	100.0(0.00)
	.5	.1	0.2(0.00)	99.6(0.02)	97.2(0.05)	98.6(0.04)
		.2	1.4(0.02)	99.9(0.01)	97.3(0.05)	99.2(0.03)
		.5	4.4(0.05)	99.8(0.01)	97.0(0.06)	100.0(0.00)
	1	.1	0.1(0.00)	99.0(0.03)	96.9(0.05)	98.2(0.04)
		.2	0.4(0.01)	99.6(0.02)	97.1(0.05)	98.7(0.04)
		.5	3.0(0.03)	99.9(0.01)	97.0(0.05)	99.6(0.02)
	2	.1	0.1(0.01)	98.4(0.04)	96.5(0.06)	97.8(0.05)
		.2	0.8(0.02)	98.4(0.04)	96.3(0.06)	98.5(0.04)
		.5	1.8(0.02)	99.5(0.02)	96.5(0.06)	99.2(0.03)
	5	.1	0.0(0.00)	98.1(0.04)	96.3(0.06)	97.4(0.05)
		.2	0.1(0.01)	99.0(0.03)	96.9(0.06)	98.3(0.04)
		.5	0.8(0.02)	99.8(0.02)	96.7(0.06)	98.8(0.03)
1000	.1	.1	2.3(0.03)	99.4(0.02)	97.8(0.05)	99.8(0.01)
		.2	-1.5(0.07)	99.9(0.01)	97.5(0.05)	100.0(0.00)
		.5	-83.2(0.11)	100.0(0.00)	100.0(0.00)	100.0(0.00)
	.5	.1	0.1(0.00)	99.4(0.02)	97.6(0.05)	98.8(0.03)
		.2	0.7(0.01)	99.8(0.02)	97.8(0.05)	99.2(0.03)
		.5	2.9(0.04)	99.3(0.03)	97.5(0.05)	99.8(0.01)
	1	.1	0.0(0.00)	99.2(0.03)	97.6(0.05)	98.6(0.04)
		.2	0.2(0.00)	99.5(0.02)	97.4(0.05)	98.8(0.03)
		.5	1.7(0.02)	99.8(0.01)	97.1(0.05)	99.2(0.03)
	2	.1	0.0(0.00)	98.6(0.04)	97.1(0.05)	98.0(0.04)
		.2	0.3(0.01)	99.0(0.03)	97.2(0.05)	98.7(0.04)
		.5	1.2(0.02)	99.1(0.03)	96.6(0.06)	98.9(0.03)
	5	.1	0.0(0.00)	98.2(0.04)	96.8(0.06)	97.7(0.05)
		.2	0.1(0.00)	99.1(0.03)	97.5(0.05)	98.6(0.04)
		.5	0.5(0.01)	99.6(0.02)	97.0(0.05)	98.7(0.04)

Table 1: Empirical bias (EBias) of \hat{x}_b and empirical coverage proportion (ECP) of \hat{x}_1^Δ , \hat{x}_1^{piv} , and \hat{x}_1^{boot} (1,000 bootstrap samples) across 100,000 simulations. Values in parentheses are empirical standard errors.

n	s	σ	Time \hat{x}_1^{piv}	Time \hat{x}_1^{boot}	Non-convergence (%)	% $\hat{x}_1^\Delta < 0$
200	.1	.1	1.01(0.00)	32.1(0.05)	8.4(0.09)	99.5(0.02)
		.2	1.02(0.00)	32.8(0.06)	26.4(0.16)	99.9(0.01)
		.5	1.02(0.00)	33.9(0.07)	41.8(0.20)	00.0(0.01)
	.5	.1	1.01(0.00)	31.7(0.05)	0.1(0.01)	15.6(0.11)
		.2	1.01(0.00)	31.9(0.05)	1.0(0.03)	62.6(0.15)
		.5	1.02(0.00)	32.2(0.05)	13.4(0.12)	99.7(0.02)
	1	.1	1.01(0.00)	31.8(0.05)	0.0(0.00)	3.7(0.06)
		.2	1.01(0.00)	31.9(0.05)	0.2(0.02)	21.1(0.13)
		.5	1.01(0.00)	32.1(0.05)	3.9(0.06)	98.6(0.04)
	2	.1	1.01(0.00)	32.1(0.05)	0.0(0.00)	0.7(0.03)
		.2	1.01(0.00)	32.1(0.05)	0.1(0.01)	10.5(0.10)
		.5	1.01(0.00)	32.1(0.05)	1.9(0.04)	78.8(0.13)
	5	.1	1.01(0.00)	32.3(0.05)	0.1(0.01)	0.4(0.02)
		.2	1.01(0.00)	32.4(0.05)	0.7(0.03)	8.1(0.09)
		.5	1.01(0.00)	32.5(0.05)	4.2(0.06)	67.8(0.15)
500	.1	.1	1.01(0.00)	31.9(0.05)	2.2(0.05)	82.3(0.12)
		.2	1.02(0.00)	32.3(0.05)	13.8(0.12)	97.8(0.05)
		.5	1.02(0.00)	33.9(0.06)	34.5(0.19)	99.7(0.02)
	.5	.1	1.01(0.00)	31.7(0.05)	0.0(0.00)	3.4(0.06)
		.2	1.01(0.00)	31.7(0.05)	0.2(0.01)	19.5(0.13)
		.5	1.01(0.00)	31.9(0.05)	4.1(0.06)	93.3(0.08)
	1	.1	1.01(0.00)	31.9(0.05)	0.0(0.00)	0.6(0.02)
		.2	1.01(0.00)	31.7(0.05)	0.0(0.01)	6.1(0.08)
		.5	1.01(0.00)	31.9(0.05)	1.0(0.03)	48.0(0.16)
	2	.1	1.01(0.00)	31.9(0.05)	0.0(0.00)	0.2(0.01)
		.2	1.01(0.00)	31.9(0.05)	0.0(0.01)	1.9(0.04)
		.5	1.01(0.00)	31.9(0.05)	0.6(0.02)	22.8(0.13)
	5	.1	1.01(0.00)	32.2(0.05)	0.1(0.01)	0.1(0.01)
		.2	1.01(0.00)	32.3(0.05)	0.3(0.02)	1.0(0.03)
		.5	1.01(0.00)	32.3(0.05)	1.8(0.04)	21.7(0.13)
1000	.1	.1	1.01(0.00)	31.8(0.05)	0.7(0.03)	31.5(0.15)
		.2	1.01(0.00)	32.1(0.05)	6.1(0.08)	86.0(0.11)
		.5	1.02(0.00)	34.3(0.07)	28.6(0.17)	98.4(0.05)
	.5	.1	1.01(0.00)	31.9(0.05)	0.0(0.00)	0.9(0.03)
		.2	1.01(0.00)	31.8(0.05)	0.1(0.01)	6.2(0.08)
		.5	1.01(0.00)	31.8(0.05)	1.5(0.04)	49.1(0.16)
	1	.1	1.01(0.00)	31.7(0.05)	0.0(0.00)	0.1(0.01)
		.2	1.01(0.00)	31.7(0.05)	0.0(0.00)	1.8(0.04)
		.5	1.01(0.00)	31.9(0.05)	0.4(0.02)	18.1(0.12)
	2	.1	1.01(0.00)	31.8(0.05)	0.0(0.00)	0.0(0.00)
		.2	1.01(0.00)	32.0(0.05)	0.0(0.00)	0.4(0.02)
		.5	1.01(0.00)	32.0(0.05)	0.3(0.02)	10.2(0.10)
	5	.1	1.01(0.00)	32.4(0.05)	0.0(0.00)	0.0(0.00)
		.2	1.01(0.00)	32.3(0.05)	0.1(0.01)	0.3(0.02)
		.5	1.01(0.00)	32.3(0.05)	1.0(0.03)	11.4(0.10)

Table 2: Average and empirical standard error of computation time for \hat{x}_1^{piv} , \hat{x}_1^{boot} relative to \hat{x}_1^Δ , proportion of non-convergent \hat{x}_b , and proportion of $\hat{x}_1^\Delta < x_0$, for 100,000 simulations.

the Delta method in this context, and a compelling reason to adopt \hat{x}_1^{piv} in its place. Further, our bootstrap lower limit \hat{x}_1^{boot} based on 1,000 samples takes only an order of magnitude more time than \hat{x}_1^Δ and \hat{x}_1^{piv} . Overall, we recommend \hat{x}_1^{piv} based on a balance of computation time and empirical coverage, although we emphasize that it is plausible that both \hat{x}_1^{piv} and \hat{x}_1^{boot} could be computed in typical applications.

5 Benchmark Dose Analysis of Prenatal Alcohol Exposure

We consider data from six longitudinal cohort studies of alcohol consumption by pregnant women conducted in Detroit (Jacobson et al., 1993), Pittsburgh (Day et al., 1991; Richardson et al., 1999), Atlanta (Coles et al., 2006; Brown et al., 1998), and Seattle (Streissguth et al., 1981). The research question of interest is to quantify levels of prenatal alcohol exposure (PAE) associated with the development of clinically important cognitive deficits in children. In these six cohort studies, children were followed from infancy through young adulthood and investigators administered a range of neuropsychological tests to assess IQ and four domains of cognitive function: learning and memory, executive function, and academic achievement in reading and mathematics. To obtain an overall cognitive function score for each children, a structural equation model was fitted for each cohort. We then used the estimated cognitive function score as the outcome measure in the analyses that follow. For details on this approach, see Jacobson et al. (submitted) and Akkaya Hocagil et al. (2023).

Data on maternal alcohol consumption were summarized in terms of average alcohol

intake per day (ounces of absolute alcohol, (AA)/day) during pregnancy, and data on a broad range of potential confounders were collected in these cohorts. Since each cohort provided a somewhat different set of confounding variables, for these data Jacobson et al. (2023) modeled the exposure variable, average alcohol intake per day, as a function of the potential confounders via linear regression model and use this to estimate a propensity score (Rosenbaum and Rubin, 1983). We used these propensity scores as covariates (Rosenbaum and Rubin, 1983; Imbens and Hirano, 2004) in the following dose-response model.

Let Y_i represent the cognitive function score, $x_i = \log(a_i + 1)$ where a_i is the average alcohol intake per day during pregnancy, $j_i \in \{1, \dots, 6\}$ index the cohort to which subject i belongs, and $z_{ij} = s_{j_i}$ denote the computed propensity scores for subject $i = 1, \dots, 2226$ in cohort j_i . A log-transformation was applied to a_i to reduce the influence of very high exposure values on the fitted model. The dose-response model is then

$$Y_i = \alpha + f(x_i) + g_{j_i}(z_{ij}) + \sigma\epsilon_i, \quad \epsilon_i \stackrel{\text{iid}}{\sim} N(0, 1), \quad (14)$$

where f is an unknown, smooth monotone dose-response function, and $g_j, j = 1, \dots, 6$ are unknown smooth functions. We apply the basis expansions of Section 2.3 and fit the model using the methods described in Section 3.2. We compute the estimated BMD, \hat{x}_b , using the method of Section 3.3, and the three candidate BMDLs, \hat{x}_1^Δ , \hat{x}_1^{piv} , and \hat{x}_1^{boot} , using the methods of Section 3.4.

Figure 1 represents the estimated dose-response curve obtained from the fitted monotone additive model along with the estimated BMD and corresponding BMDLs. The estimated BMD for $p_0 = 0.025$ and $p_+ = 0.01$ was $\hat{x}_b = 1.00$ and the three BMDLs were $\hat{x}_1^{\text{piv}} = 0.236$,

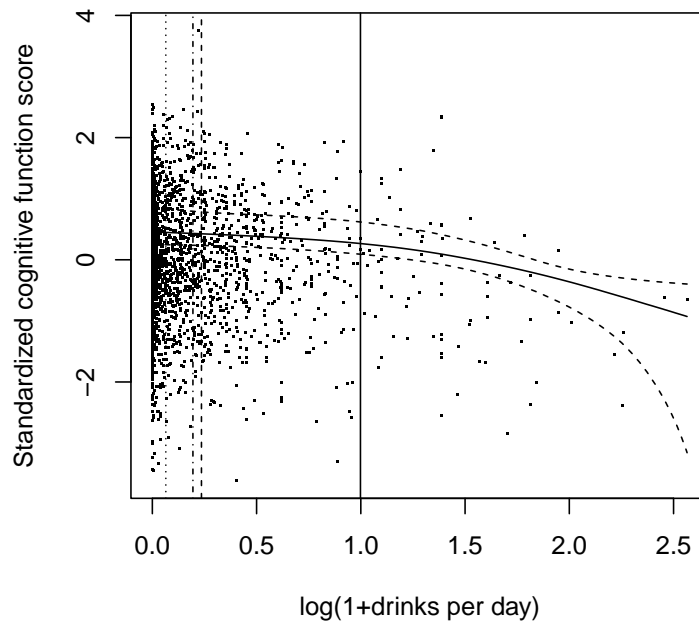
$\hat{x}_1^{\text{boot}} = 0.195$, and $\hat{x}_1^\Delta = 0.065$. The Delta method estimate, \hat{x}_1^Δ , is much closer to zero than the other two, and hence communicates a much more conservative clinical recommendation; combined with its empirical coverage being too high in simulations, we remark that this can be regarded as a disadvantage of the Delta method over the two proposed BMDLs. The conclusion based on \hat{x}_1^{piv} is that expectant mothers should consume not more than $\exp(0.236) - 1 = 0.266$ oz of absolute alcohol which corresponds to approximately 0.45 standard drinks per day, on average, to avoid clinically significant cognitive defects in their children.

The total amount of time that the procedure took to fit the model, estimate the BMD, and compute the three BMDLs based on 100,000 bootstrap iterations was 396 seconds on a 2021 M1 Macbook Pro with 64Gb of RAM. Model fitting and estimating the BMD took 3.93 seconds and 30 microseconds, respectively. The computation time for 100,000 iterations of the parametric bootstrap for \hat{x}_b was the longest at 390 seconds, and produced a result close to \hat{x}_1^{piv} which was computed nearly $1000\times$ faster in only 0.4 seconds. Without running the bootstrap, the procedure would have taken a total of 5.53 seconds to perform a full semi-parametric benchmark dose analysis on these data.

6 Discussion

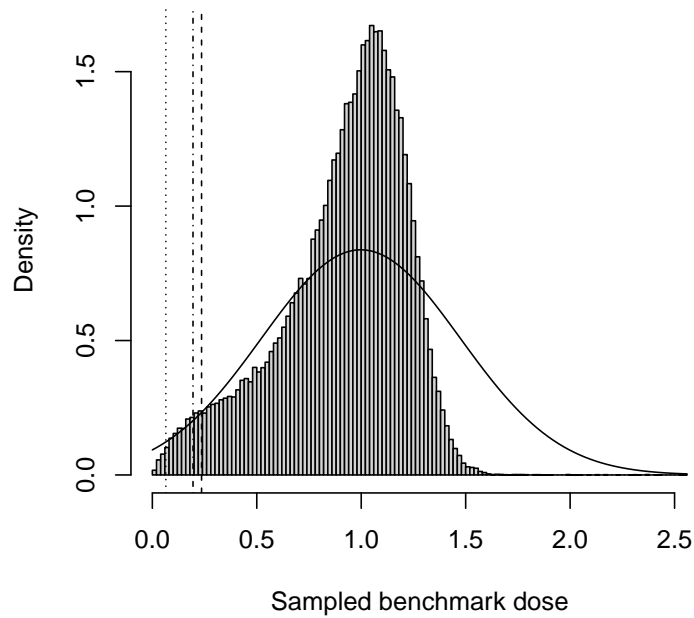
We recommend avoiding the Delta method (\hat{x}_1^Δ ; Section 3.4.2) for forming confidence intervals for \hat{x}_b in general. The estimate \hat{x}_b is a highly non-linear function of the MLE, and should not be expected to have a sampling distribution that is close to Gaussian. An example of this is shown in Figure 1 (b) for the PAE data analysis, in which the approximate

Dose-response curve, cog. score vs drinks/day



(a) Estimated dose-response curve, f .

Posterior dist. of the BMD, 100,000 samples



(b) Posterior samples of the benchmark dose, x_b

Figure 1: (a) Estimated dose-response curve \hat{f} and uncertainty bands computed as point-wise 95% credible intervals from 100,000 samples from the posterior of the fitted curve (- -

posterior distribution of \hat{x}_b is extremely non-normal, leading to a substantial overestimation of uncertainty and a low value of \hat{x}_1^Δ .

The estimated dose-response curve shown in Figure 1 (a) for the PAE data analysis is very flat at low exposure values. This appears to be due to a large amount of noise relative to signal in the PAE data themselves, suggesting that a single exposure may not be sufficiently informative (Jacobson et al., 2023). Akkaya Hocagil et al. (2023) performs a benchmark dose analysis for PAE using a bivariate exposure that incorporates both frequency and severity of drinking. In future work we plan to develop an efficient computational method for the semi-parametric bivariate exposure case, making use of the fast computational methods developed in the present manuscript to improve the practical application of benchmark dose estimation with bivariate exposure.

Although the present paper presents methodology that is specifically tied to computations related to benchmark dose estimation and its associated lower confidence limit, there is potential for the methods to apply in more general settings. In particular, it is useful to recognize that estimating a benchmark dose represents a specific example of a broader class of inverse estimation problems, where the object of interest is a point on the x -axis in a semi-parametric regression model, and is hence obtained by solving a random nonlinear equation. Inverse problems arise in a wide range of applied settings, for example, chemical calibration or medical imaging, and it would be interesting to apply similar approaches to those used in the present paper in other such problems.

References

- Aerts, M., Wheeler, M. and Cortinas Abrahantes, J. (2020). An extended and unified modeling framework for benchmark dose estimation for both continuous and binary data. *Environmetrics*, 31.
- Akkaya Hocagil, T. et al (2023). Benchmark dose profiles for bivariate exposures. *Submitted*.
- Astley, S.J. and Clarren, S.K. (2000). Diagnosing the Full Spectrum of Fetal Alcohol-Exposed Individuals: Introducing the 4- Digit Diagnostoc Code. *Alcohol and Alcoholism*, 35(4):400–410.
- Brown, J., Bakeman, R., Coles, C., Sexson, W. and Demi, A. (1998). Maternal drug use during pregnancy: are preterm and full-term infants affected differently? *Dev Psychol.*, 34:540–554.
- Budtz-Jorgensen, E., Keiding, N. and Grandjean, P. (2001). Benchmark Dose Calculation from Epidemiological Data. *Biometrics*, 57:698–706.
- Chudley, A.E., Conry, J., Cook, J.L., Looock, C., Rosales, T. and LeBlanc, N. (2005). Fetal alcohol spectrum disorder: Canadian guidelines for diagnosis. *CMAJ*, 172(5 suppl):S1–S21.
- Coleman, T.F. and Li, Y. (1994). On the convergence of interior-reflective Newton methods for nonlinear minimization subject to bounds. *Mathematical Programming*, 67:189–224.
- Coles, C., Platzman, K., Raskind-Hood, C., Brown, R., Falek, A. and Smith, I. (2006). A comparison of children affected by prenatal alcohol exposure and attention deficit, hyperactivity disorder. *Alcoholism: Clinical and Experimental Research*, 21:150 – 161.

- Cook, J.L. et al (2016). Fetal alcohol spectrum disorder: a guideline for diagnosis across the lifespan. *CMAJ*, 188(3):191–197.
- Crump, K. (1984). A New Method for Determining Allowable Daily Intakes. *Fundamental and Applied Toxicology*, 4:854–871.
- Crump, K. (1995). Calculation of Benchmark Doses from Continuous Data. *Risk Analysis*, 15(1).
- Day, N. et al (1991). Prenatal marijuana use and neonatal outcome. *Neurotoxicology and Teratology*, 13(3):329 – 334.
- de Boor, C. (2001). *A Practical Guide to Splines*. Applied Mathematical Sciences. Revised edition edition.
- Eddelbuettel, D. and Francois, R. (2011). Rcpp: Seamless R and C++ Integration. *Journal of Statistical Software*, 40(8):1–18.
- EFSA, S.C. et al (2022). Guidance on the use of the benchmark dose approach in risk assessment. *EFSA Journal*, 20(10):e07584.
- EPA, U. (2012). Benchmark Dose Technical Guidance.
- Haber, L.T. et al (2018). Benchmark dose (BMD) modeling: current practice, issues, and challenges. *Critical Reviews in Toxicology*, 48(5):387–415.
- Hoyme, H. et al (2016). Updated clinical guidelines for diagnosing fetal alcohol spectrum disorders. *Pediatrics*, 138:e20154256–e20154256.

- Hoyme, H.E. (2005). A Practical Clinical Approach to Diagnosis of Fetal Alcohol Spectrum Disorders: Clarification of the 1996 Institute of Medicine Criteria: In Reply. *Pediatrics*, 115(6):1787–1788.
- Imbens, G. and Hirano, K. (2004). The propensity score with continuous treatments.
- Jacobson, J. et al (2023). Effects of Prenatal Alcohol Exposure on Cognitive Development: A Dose-response Analysis. *Submitted*.
- Jacobson, J.L., Jacobson, S.W., Sokol, R.J., Martier, S.S., Ager, J.W. and Kaplan-Estrin, M.G. (1993). Teratogenic effects of alcohol on infant development. *Alcoholism: Clinical and Experimental Research*, 17(1):174–183.
- Kristensen, K., Nielson, A., Berg, C.W., Skaug, H. and Bell, B.M. (2016). TMB: automatic differentiation and Laplace approximation. *Journal of Statistical Software*, 70(5).
- Lin, L., Piegorsch, W. and Bhattacharya, R.N. (2015). Nonparametric Benchmark Dose Estimation with Continuous Dose-Response Data. *Scandinavian Journal of Statistics*, 42:713–731.
- Moerbeek, M., Piersma, A.H. and Slob, W. (2004). A Comparison of Three Methods for Calculating Confidence Intervals for the Benchmark Dose. *Risk Analysis*, 24(1).
- Piegorsch, W., Xiong, H., Bhattacharya, R.N. and Lin, L. (2012). Nonparametric estimation of benchmark doses in environmental risk assessment. *Environmetrics*, 23:717–728.
- Piegorsch, W., Xiong, H., Bhattacharya, R.N. and Lin, L. (2014). Benchmark Dose Analysis via Nonparametric Regression Modeling. *Risk Analysis*, 34(1).

- Pya, N. and Wood, S.N. (2015). Shape constrained additive models. *Statistics and Computing*, 25:543–559.
- Richardson, G., Hamel, S., Goldschmidt, L. and Day, N. (1999). Maternal drug use during pregnancy: are preterm and full-term infants affected differently? *Pediatrics*, 104.
- Rosenbaum, P.R. and Rubin, D.B. (1983). The central role of the propensity score in observational studies for causal effects. *Biometrika*, 70:41–55.
- Rue, H. (2001). Fast sampling of Gaussian Markov random fields. *Journal of the Royal Statistical Society, Series B: Statistical Methodology*, 63(2):325–338.
- Stratton, K., Howe, C. and Battaglia, F.C. (1996). *Fetal Alcohol Syndrome: Diagnosis, Epidemiology, Prevention, and Treatment*. The National Academies Press, Washington, DC.
- Streissguth, A., Martin, D., Martin, J. and Barr, H. (1981). The seattle longitudinal prospective study on alcohol and pregnancy. *Neurobehav Toxicol Teratol*, 2(3):223–233.
- Stringer, A. (2023). Identifiability constraints in generalized additive models. *Canadian Journal of Statistics*, Accepted.
- Wheeler, M. and Bailer, A.J. (2012). Monotonic Bayesian Semiparametric Benchmark Dose Analysis. *Risk Analysis*, 32(7).
- Wheeler, M., Shao, K. and Bailer, A.J. (2015). Quantile benchmark dose estimation for continuous endpoints. *Environmetrics*, 26:363–372.

Wood, S. (2011). Fast stable restricted maximum likelihood and marginal likelihood estimation of semiparametric generalized linear models. *Journal of the Royal Statistical Society, Series B (Statistical Methodology)*, 73(1):3 – 36.

Wood, S. (2017). P-splines with derivative based penalties and tensor product smoothing of unevenly distributed data. *Statistics and Computing*, 27:985–989.

Wood, S., Pya, N. and Säfken, B. (2016). Smoothing parameter and model selection for general smooth models. *Journal of the American Statistical Association*, 111:1548 – 1575.

A Algorithms

Algorithm 1 de Boor’s Algorithm for Spline Curve Evaluation

Require: $x \in \mathbb{R}, \boldsymbol{\beta} = (\beta_1, \dots, \beta_L), p \in \mathbb{N}, \mathbf{t} = (t_1, \dots, t_{L+p})$ such that $f(x) = \sum_{l=1}^L b_{l,p}(x)\beta_l$.
 Define $k : x \in [t_k, t_{k+1})$
for $j = 0, \dots, p - 1$ **do** $\beta_j^* = \beta_{j+k-(p-1)}$
end for
for $r = 1, \dots, p - 1$ **do**
 for $j = (p - 1), \dots, r$ **do**
 $\mathbf{a} = (x - t_{j+k-(p-1)}) / (t_{j+1+k-r} - t_{j+k-(p-1)})$
 $\beta_j^* = (1 - \mathbf{a})\beta_{j-1}^* + \mathbf{a}\beta_j^*$
 end for
end for
return $\beta_{p-1}^* = f(x)$

Algorithm 2 Reflective Newton Line-Search for Benchmark Dose Estimation

Require: $\widehat{\beta}_c$ re-parameterized estimated spline weights; \mathbf{t} spline knots; $\widehat{\sigma} > 0, c(p_0, p_+), \epsilon > 0, p = 4, x_0 < x_{\max}$
Let $t = 0, x^0 = (x_0 + x_{\max})/2, \mathbf{u} = 1 + \epsilon, \mathbf{u}' = 1$.
 $\mathbf{f}_0 = \text{deBoor}(x_0, \widehat{\beta}_c, \mathbf{t}, p)$
Let $\widehat{\beta}'_c = \left\{ (p-1)(\widehat{\beta}^c_i - \widehat{\beta}^c_{i-1}) / (t_{i+p-1} - t_i) \right\}_{i=2}^L$
while $|\mathbf{u}| > \epsilon$ **do**
 $\mathbf{f} = \text{deBoor}(x^t, \widehat{\beta}_c, \mathbf{t}, p), \mathbf{f}' = \text{deBoor}(x^t, \widehat{\beta}'_c, \mathbf{t}, p-1)$
 $\mathbf{u} = (\mathbf{f}_0 - \mathbf{f}) / \widehat{\sigma} - c(p_0, p_+), \mathbf{u}' = -\mathbf{f}' / \widehat{\sigma}$
 $x^{t+1} \leftarrow x^t - \mathbf{u} / \mathbf{u}'$
 $x^{t+1} \leftarrow \text{Reflect}(x^{t+1}, x_0, x_{\max})$
 $t \leftarrow t + 1$
end while
 return $\widehat{x}_b = x^{t+1}$

Require: $\text{Reflect}(x, l, u) = \min(w, 2(u-l) - w) + l$, where $w = |y-l| \bmod \{2(u-l)\}$.

Require: $\text{deBoor}(x, \beta, \mathbf{t}, p)$: Algorithm 1

Algorithm 3 Reflective Newton Line-Search for Benchmark Dose Lower Limit Computation

Require: $\widehat{\beta}_c$ re-parameterized estimated spline weights; \mathbf{t} spline knots; $\widehat{\sigma} > 0, c(p_0, p_+), \epsilon > 0, p = 4, x_0 < \widehat{x}_b; \Sigma(\widehat{\beta})$ variance matrix; $0 < \alpha < 1, q : P(\chi_1^2 < q) = \alpha$.
Let $t = 0, x^0 = (x_0 + \widehat{x}_b)/2, \mathbf{psi} = 1 + \epsilon, \mathbf{psi}' = 1$
Let $\widehat{\beta}'_c = \left\{ (p-1)(\widehat{\beta}^c_i - \widehat{\beta}^c_{i-1}) / (t_{i+p-1} - t_i) \right\}_{i=2}^L$
while $|\mathbf{u}| > \epsilon$ **do**
 $\mathbf{f} = \text{deBoor}(x^t, \widehat{\beta}_c, \mathbf{t}, p), \mathbf{f}' = \text{deBoor}(x^t, \widehat{\beta}'_c, \mathbf{t}, p-1)$
 $\mathbf{u} = (\mathbf{f}_0 - \mathbf{f}) / \widehat{\sigma} - c(p_0, p_+), \mathbf{u}' = -\mathbf{f}' / \widehat{\sigma}, \mathbf{v} = V_n(x^t), \mathbf{v}' = V'_n(x^t)$
 $\mathbf{psi} = \mathbf{u}^2 - \mathbf{v}q, \mathbf{psi}' = 2\mathbf{u}\mathbf{u}' - \mathbf{v}'q$
 $x^{t+1} \leftarrow x^t - \mathbf{psi} / \mathbf{psi}'$
 $x^{t+1} \leftarrow \text{Reflect}(x^{t+1}, x_0, \widehat{x}_b)$
 $t \leftarrow t + 1$
end while
 return $\widehat{x}_1^{\text{pi}v} = x^{t+1}$

Require: $\text{Reflect}(x, l, u) = \min(w, 2(u-l) - w) + l$, where $w = |y-l| \bmod \{2(u-l)\}$.

Require: $\text{deBoor}(x, \beta, \mathbf{t}, p)$: Algorithm 1.
